Burgess, S. K., Trimmer, P. A., & McCarthy, K. (1985) *Brain Res. 335*, 11-19.
Burns, C. P., & Dudley, D. T. (1982) *Biochem. Pharmacol. 31*, 2116-2119.
Chapman, D. (1975) *Biomembranes 7*, 1-9.
Dawidowicz, E. A. (1987) *Annu. Rev. Biochem. 56*, 43-61.
Golan, D. E., Brown, C. S., Cianci, C. M. L., Furlong, S. T., & Caulfield, J. P. (1986) *J. Cell Biol. 103*, 819-828.
Hartley, H. O. (1961) *Technometrics 3*, 269-280.
Hoffman, R. D., Kligerman, M., Sundt, T. M., Anderson, N. D., & Shin, H. S. (1982) *Proc. Natl. Acad. Sci. U.S.A. 79*, 3285-3289.
Kuby, S. A., Node, L., & Lardy, H. A. (1954) *J. Biol. Chem. 209*, 191.
Lands, W. E. M. (1960) *J. Biol. Chem. 235*, 2233-2237.
Melchior, D. L., & Stein, J. M. (1976) *Annu. Rev. Biophys. Bioeng. 5*, 205-237.
Mohandras, N., Wyatt, J., Mel, St. F., Rossi, M. E., & Shohet, St. B. (1982) *J. Biol. Chem. 257*, 6537-6543.
Quinn, M. T., Parthasarathy, S., & Steinberg, D. (1988) *Proc. Natl. Acad. Sci. U.S.A. 85*, 2805-2809.
Rule, G. S., Law, P., Kruuv, J., & Lepock, J. R. (1980) *J. Cell Physiol. 103*, 407-416.
Ryan, J., & Simoni, R. D. (1980) *Biochim. Biophys. Acta 598*, 606-615.
Savard, J. D., & Choy, P. C. (1982) *Biochim. Biophys. Acta 711*, 40-48.
Shirazi, M. F., Aronson, N. N., & Dean, R. T. (1982) *J. Cell Sci. 57*, 115-127.
Tamura, A., Tanaka, T., Yamana, T., Nasu, R., & Fujii, T. (1985) *J. Biochem. (Japan) 97*, 353-359.
van den Bosch, H. (1982) *Phospholipids* (Hawthorne, J. N., & Ansell, G. B., Eds.) Chapter 9, Elsevier Biomedical Press, Amsterdam.
Weigel, P. H., & Oka, J. A. (1981) *J. Biol. Chem. 256*, 2615-2617.

Structural Elements of Human Parathyroid Hormone and Their Possible Relation to Biological Activities†

W. Neugebauer, W. K. Surewicz,* H. L. Gordon, R. L. Somorjai, W. Sung, and G. E. Willick*
Protein Structure and Function Section, Institute for Biological Sciences, National Research Council of Canada, Ottawa, Canada K1A OR6

Received July 29, 1991; Revised Manuscript Received October 28, 1991

ABSTRACT: Human parathyroid hormone (hPTH) and several deletion analogues were examined for the presence of secondary structure using circular dichroism spectroscopy. The spectra of hPTH and the deletion analogues 8-84, 34-53, 53-84, 1-34, 13-34, 1-19, and 20-34, in neutral, aqueous buffer, gave no evidence for extensive secondary structure. An α-helical-like spectral contribution was found to arise from a region within peptide 13-34. This spectral contribution was speculated to arise from partial stability of a helix consisting of residues 17-29. Molecular dynamics simulations of peptide 1-34 suggested that this peptide tends to fold with a bend defined by residues 10-14, with the amino-terminal and carboxyl-terminal residues tending to be in more extended forms and the other residues in helical-like conformations. The addition of trifluoroethanol promoted the formation of α-helix, mainly in the 1-34 region. The putative helix comprised of residues 17-29 was stabilized by the addition of 10-20% TFE, while a second putative helix proximal to the amino terminus, and comprised of residues 3-11, was stabilized by slightly higher concentrations of TFE. An amphiphilic sequence was identified within the 20-34 fragment. The development of α-helix on binding this fragment, and other analogues containing this sequence, to palmitoyloleoylphosphatidylserine vesicles provided experimental evidence for the potential role of this amphiphilic sequence in binding to membranes or to a membrane receptor. The relationships between these α-helical regions in 1-34, either potentiated by trifluoroethanol or lipid vesicles, are discussed in terms of different receptor-binding regions within hPTH.

Parathyroid hormone (PTH)[1] plays a major role in regulating circulating calcium levels through effects on the kidney and on resorption and deposition of calcium in bone. The full-sized hormone is 84 residues long and has recently become available in quantities as a result of expression of the gene in *Escherichia coli* (Hogset et al., 1990; Sung et al., 1991). However, almost all of the reported in vitro activities require only sequences within the 1-34 segment, and consequently this is the region about which most studies have centered.

The biological activity of hPTH has been monitored extensively by measuring adenylate cyclase activation and by radioreceptor assays using kidney or bone tissue or cultured cells (Jüppner, 1989). In these two assays, PTH and the 1-34 fragments are equally active. For stimulation of adenylate cyclase, almost all of the 1-34 sequence is required, including the NH_2-terminal serine or alanine. In contrast, a recently reported mitogenic effect (Schlüter et al., 1989) and a stimulation of protein kinase C activity (Jouishomme et al., 1992)

† This is National Research Council of Canada Publication No. NRC 31986.
* Authors to whom correspondence should be addressed.

[1] Abbreviations: PTH, human parathyroid hormone; hPTH, human PTH; CD, circular dichroism; TFE, trifluoroethanol; POPS, 1-palmitoyl-2-oleoylphosphatidylserine.

0006-2960/92/0431-2056$03.00/0 Published 1992 by the American Chemical Society

were shown to require a short sequence within the 1–34 fragment.

There have been contradictory reports on the amount of secondary structure in PTH(1–34) in aqueous solution. In an early circular dichroism (CD) study (Epand et al., 1985) and a recent NMR study (Lee & Russell, 1989), little or no secondary structure was indicated. However, another CD study (Zull et al., 1990) and an NMR study (Smith et al., 1987) have suggested the presence of some ordered secondary structure within this fragment.

In this paper, we examine the structure of human PTH (hPTH) and several deletion analogues using CD spectroscopy, predictive algorithms, and molecular dynamics simulations. These data point to sequence regions within hPTH that either have α-helical-like structure in aqueous buffer at neutral pH or that form a helix in the presence of increasing amounts of a helix-promoting solvent. Furthermore, the presence of an amphiphilic helix in the sequence region important for binding to at least one type of PTH receptor is demonstrated.

Materials and Methods

Recombinant hPTH. hPTH(1–84) and the 8–84 analogue were expressed in *E. coli* and purified as previously described (Sung et al., 1991).

Synthetic PTH Analogues. hPTH(1–34), 13–34, and 53–84 were obtained from Bachem (Torrance, CA). Analogue 34–53 was synthesized as the amide on a methylbenzhydrylamine resin using *t*-Boc chemistry (Stewart & Young, 1984). Analogoues 1–19 and 20–34 were synthesized by FMOC chemistry (Fields & Noble, 1990) on a Rink amide support (Amino Tech, Ottawa, Canada) (Rink, 1987; Sieber, 1987). Peptides were purified by HPLC and correct products identified by amino acid analysis and mass spectroscopy.

Circular Dichroism Spectroscopy. Spectra were obtained on a JASCO J-600 spectropolarimeter at 20–22 °C. Typically, four spectra were averaged, and the spectra were smoothed by the software provided by JASCO. The instrument was calibrated with ammonium D-camphorsulfonate. Concentrations of the peptides were obtained either from the absorption at 280 nm, using an extinction coefficient of 5700 M^{-1} for the single tryptophan, or by amino acid analysis using norleucine as an internal standard.

Preparation of Palmitoyloleoylphosphatidylserine (POPS) Vesicles. Small unilamellar POPS vesicles (Avanti Polar Lipids) were prepared by suspending the lipid in buffer (20 mM Hepes, 100 mM NaCl, pH 7.2). The suspension of about 15 mg/mL lipid was sonicated in an ice bath for about 15 min using a probe-type sonifer. Metal debris from the titanium tip was removed by centrifugation for 10 min in a microfuge. Vesicles were kept at room temperature and used within a few hours after preparation.

Molecular Dynamics Simulations. Molecular dynamics (MD) simulations of 1–34 and 20–34 hPTH were performed using the CHARMM package, version 21.2, Polygen Corp. (Brooks et al., 1983). All atoms, including hydrogens, were modeled explicitly, and all nonbonded interactions were included in the computation of the potential energy. The solvent was modeled as a dielectric continuum, i.e., electrostatic interactions were screened via a dielectric function $\epsilon(r) = \epsilon_b r$, where r is the interatomic distance, and with ϵ_b chosen to be 78 or 2. All simulations were done at 300 K with a time step of 0.001 ps. Covalent bonds to hydrogen were constrained by SHAKE to their equilibrium distances (van Gunsteren et al., 1977). Data were collected over a period of 2–3 ns for the 20–34 fragment and 0.5 ns for the 1–34 fragment, after a suitable equilibration period. Secondary structure analysis was done with QUANTA softwear (Polygen Corp.).

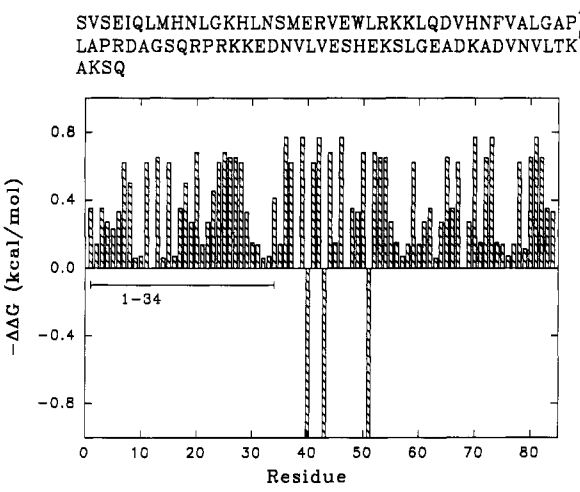

FIGURE 1: Predicted helical regions in hPTH. Helical tendencies for residues of hPTH are plotted on the basis of a thermodynamic scale (O'Neill & DeGrado, 1990). The sequence of hPTH is shown above in the single-letter code for amino acids.

Results

Secondary Structure Prediction for hPTH(1–84). The α-helical tendencies for the residues of hPTH, based on the thermodynamic scale of O'Neil and DeGrado (1990), are shown in Figure 1. This scale is probably more appropriate for these polypeptide sequences than the commonly used predictive algorithms based on the secondary structure probabilities of amino acid residues in globular proteins. The midregion of the molecule, residues 39–52, is not predicted to form any helical structure. However, the flanking regions, which include the carboxyl and amino termini, do show potential to form α-helices. Within the biologically active sequence, 1–34, there are two regions, 1–8 and 17–29, which are predicted to be α-helical. The predictive algorithm of Chou and Fasman (1974) gave similar results, but the thermodynamic scale gave more emphasis to a helix including residues 17–29. The Chou–Fasman β-turn algorithm (Chou & Fasman, 1977) predicted turns near the middle of hPTH. The most strongly predicted was the sequence DAGS[48]. Within the biologically active sequence 1–34, three sequences were weakly predicted as possible β-turns, NLGK[13], GKHL[15], and HLNS[17].

Far-UV CD Analyses. The CD spectra of hPTH and several deletion analogues in neutral aqueous buffer were examined for possible indications of secondary structure. The spectra of the 53–84, and especially the 34–53 fragments, with pronounced minima at 195–197 nm, are typical of polypeptides with little or no defined secondary structure (Figure 2A). In contrast, hPTH(1–34) and some fragments of it have a pronounced minimum at 220 nm, indicative of the presence of some ordered secondary structure (Figure 2B). Additionally, the spectrum of hPTH was found to be approximated by the sum of the spectra of fragments 1–34, 34–53, and 53–84. These observations imply that most of the ordered secondary structure in hPTH lies within the 1–34 region. The minimum observed at about 220 nm in the spectra of hPTH and fragments 1–34 and 13–34 is largely absent in fragments 1–19 and 20–34. This suggests that any structure present includes, in part, residues within 13–19.

The commonly used algorithms for analyzing secondary structure from CD data rely on basis spectra derived from proteins with well-characterized structures from X-ray crystallographic data. However, their use is questionable for

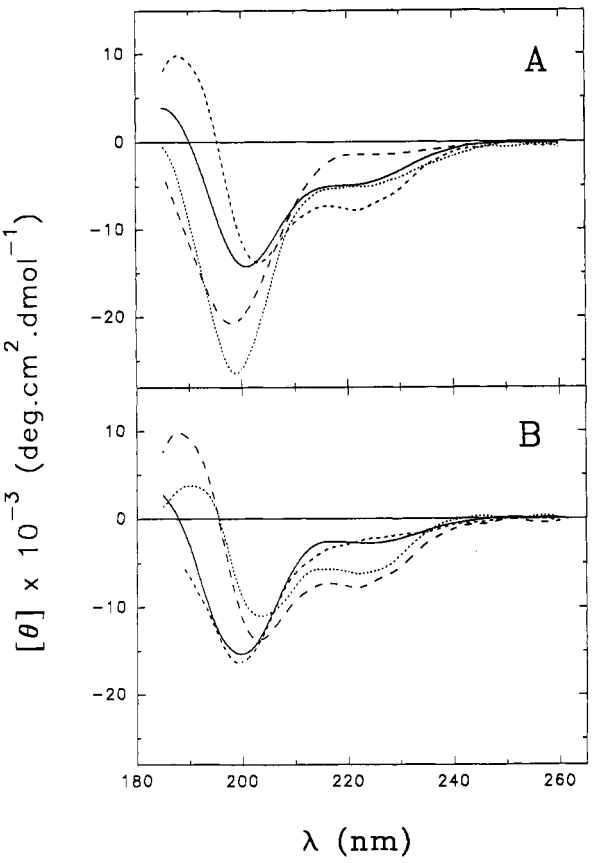

FIGURE 2: CD spectra of hPTH and deletion analogues in aqueous buffer. Spectra were taken in 25 mM sodium phosphate, pH 7.2 (A) 1–84 (—), 1–34 (---), 34–53 (– – –), and 53–84 (•••). (B) 1–19 (—), 20–34 (---), 1–34 (– – –), and 13–34 (•••).

Table I: Helical Residues in PTH Analogues

	number of residues in α-helix[a]					
% TFE	1–84	8–84	1–34	1–19	20–34	13–34
0	15	11	9	–[b]	–	5
10	26	18	15	–	–	7
20	27	31	20	9	6	13
40	49	37	26	13	8	15

[a] α-Helix was estimated from $[\theta]_{222}$ values, using the equation $n = ([\theta]_{222}^{obs}/[\theta]_{222}^{10})N$, where $[\theta]_{222}^{obs}$ = observed ellipticity at 222 nm, $[\theta]_{222}^{10}$ = ellipticity value of 28 000 deg·cm²·dmol⁻¹ for a helix of length 10 at 222 nm, from the data of Yang et al. (1986), N = peptide length, and n = number of residues in helix. [b] The calculated value is ≤4.0.

molecules such as PTH. PTH has a CD spectrum suggestive of a large amount of "random" coil, with a hint of some secondary structure indicated by the presence of a weak minimum near 220 nm. The FTIR spectrum of hPTH gave no indication of the presence of β-sheet (data not shown). A type I β-turn could conceivably contribute to the type of CD spectra observed with hPTH and some of its analogues (Bandekar et al., 1982). However, as described below, no evidence was found in the molecular dynamics simulations for the presence of such a specific turn configuration. Random coils, as exemplified by the 34–53 fragment, have little ellipticity at 220 nm. These considerations make an α-helix the only likely source of the minimum in this region, that is in addition to the small coil contribution. Therefore, we have estimated the amount of residues in an α-helical configuration from the magnitude of the 220-nm minimum in the specific ellipticity, using a value of 28 000 deg·cm²·dmol⁻¹ for a peptide 10 residues in length (Yang et al., 1986) (Table I). As the helix length decreases, and as the relative contribution of the coil increases, these estimated values become increasingly uncertain. Thus, we have

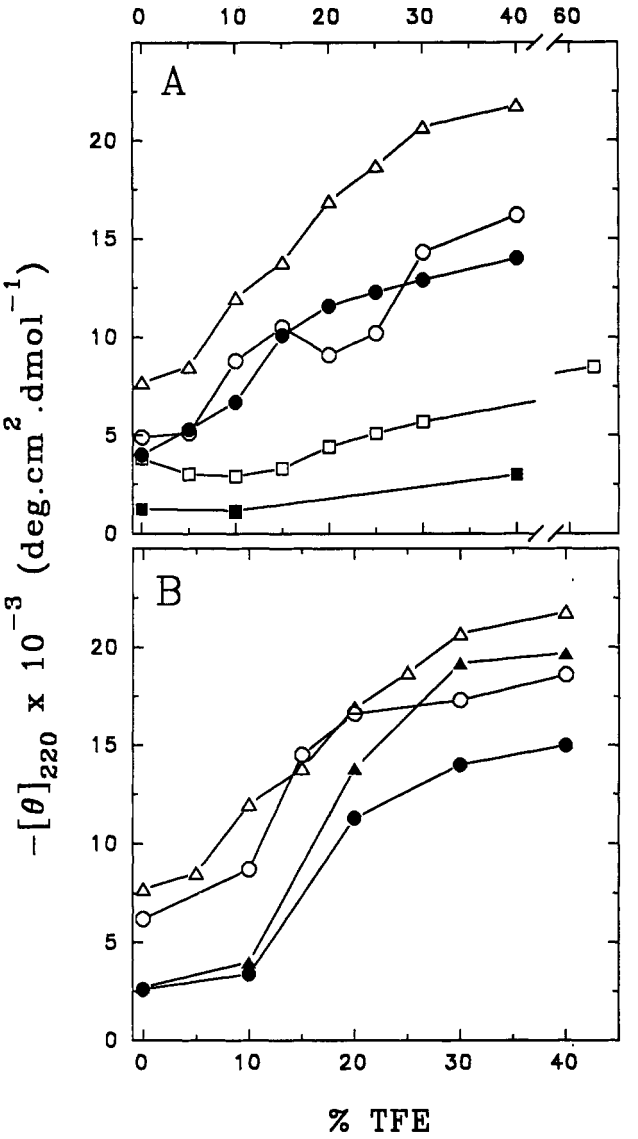

FIGURE 3: Development of helix in PTH analogues on addition of TFE. Plots are of $[\theta]_{220}$ as a function of TFE concentration in 25 mM sodium phosphate, pH 7.2. (A) 1–34 (△), 1–84 (○), 8–84 (●), 34–53 (■), and 53–84 (□). (B) 1–34 (△), 13–34 (○), 1–19 (▲), and 20–34 (●).

chosen to discount from the analyses calculated values for the number of helical residues which are 4 or less.

Trifluoroethanol (TFE) promotes the formation of α-helices in polypeptides. The extent of formation of helix in a particular peptide is related to the propensity of the peptide to form a stable helix. Plots of $[\theta]_{220}$ at increasing concentrations of TFE showed that fragment 1–34, hPTH, and hPTH(8–84) had relatively strong propensities to form helical structures (Figure 3A). Fragment 53–84 showed some tendency to form a helical structure, but only at the higher TFE concentrations. In contrast, 34–53 formed no helical structure even at the highest TFE concentrations studied. From these data, estimates of the number of residues in each peptide showed that most of the helical structure in hPTH at up to 20% TFE was present in the 1–34 region (Table I).

Further examination of fragments of peptide 1–34 showed that most of the helix formed in this region lay within the 13–34 sequence (Figure 3B, Table I). Fragments 1–19 and 20–34 both formed helical structure, but mainly above 20% TFE. The formation of most of the helical structure in fragment 13–34 at less than 20% TFE again suggested that a region with a strong propensity to form a helix exists within

Table II: Cluster Center Analysis of Molecular Dynamics Simulation of PTH(20–34)

run	cluster	f^a	R	V	E	W	L	R	K	K	L	Q	D	V	H	N	F
A[b]	1	0.62	r	3	3	f	f	f	r	f	4	4	4	5	5	4	4[c]
	2	0.38	r	r	f	4	4	4	5	5	5	5	f	4	4	4	r
B[d]	1	0.14	r	h	h	h	h	h	5	5	f	r	4	4	4	r	r
	2	0.53	r	h	h	h	h	h	5	f	f	r	4	4	4	5	r
	3	0.33	r	4	4	4	5	5	5	5	r	r	h	h	h	h	r
C[e]	1	1.00	r	r	r	r	r	r	r	r	r	r	r	4	4	4	r
D[f]	1	0.64	r	3	h	h	h	h	h	h	h	r	r	r	r	r	r
	2	0.36	r	r	r	h	h	h	h	h	h	5	r	r	r	r	r

[a] f, fraction of conformers in cluster. [b] Run initiated from a helical starting conformation, $\epsilon_b = 78$. Data were collected for 2 ns after a 0.4-ns equilibration. [c] The polypeptide conformation of residues of cluster centers designated by QUANTA is indicated as r, unassigned; f, fold (C_α torsion helical); 3, 3-turn (H-bond between i and i+3 residues); 4, 4-turn (H-bond between i and i+4 residues); h, α-helix (>3 consecutive 4-turns); 5, 5-turn (H-bond between i and i+5 residues). Three or more consecutive equivalent elements have been underlined. [d] The run was initiated from randomized starting conformation, $\epsilon_b = 78$. Data were collected for 3 ns after a 0.35-ns equilibration. [e] The run was initiated from extended starting conformation, $\epsilon_b = 78$. Data were collected for 2 ns after a 0.4-ns equilibration. [f] The run was initiated from randomized starting conformation, $\epsilon_b = 2$. Data were collected for 2 ns after a 0.05-ns equilibration.

Table III: Cluster Center Analysis of Molecular Dynamics Simulation of PTH(1–34)

run	cluster	f	S V S E I Q L M H N L G K H L N S M E R V E W L R K K L Q D V H N F
A[a]	1	0.23	r h h h h h h h h h h h h 5 h h h h h h h h h h h h h h h h h r[b]
	2	0.77	r r r h h h h h h 5 h h h h 5 4 4 4 5 h h h h 5 h h h h h h h r r
B[c]	1	1.00	r h h h h h h h h h h h h h h h h h h h h h h h h h h h h h h r

[a] The run was initiated from a helical starting conformation, $\epsilon_b = 78$. Data were collected for 0.5 ns after a 0.05-ns equilibration. [b] The polypeptide conformation of the residues of the cluster center is as indicated in Table II. [c] The run was initiated from a helical starting conformation, $\epsilon_b = 2$. Data were collected for 0.45 ns after a 0.07-ns equilibration.

this sequence and that the NH_2-terminal region of this helix lies within residues 13–19. Although these data on TFE stabilization cannot be readily understood in terms of a physical model, they do provide characteristic data on the analogues that could be useful in terms of aiding future analogue studies.

Near-UV CD Spectra. The near-UV CD spectra of peptides and proteins reflect the asymmetries of the environments of the aromatic residues, and particularly that of tryptophan and tyrosine. In hPTH, the near-UV spectrum is expected to arise predominantly from the transitions of the single Trp-23. Spectra were taken of hPTH and analogues 13–34 and 20–34 in increasing concentrations of TFE. Each of these spectra showed no further change above concentrations of TFE which were peculiar to the each peptide (Figure 4). This suggests that for each peptide the tryptophan lies in a fixed environment when the TFE concentration reaches a particular level. The most reasonable explanation for this is that the tryptophan in each case lies within an α-helix stabilized by the TFE. At the TFE concentrations for each peptide indicated in Figure 4, the approximate number of residues in an α-helix in each of hPTH and fragments 13–34 and 20–34 is 26, 13, and 8, respectively. This suggests that a sequence including Trp-23, beginning within residues 13–19 and extending into the 20–34 region, is the first one stabilized as an α-helix at low concentrations of TFE.

The near-UV spectrum of hPTH in the presence of TFE was similar in magnitude and shape to that of 13–34, but distinctly different from that of peptide 20–34 (Figure 5). The helix within peptide 20–34 in 40% TFE is estimated to be only about eight residues long (Table I), and the thermodynamic prediction suggests that the most likely sequence for this helix includes residues Glu-22–Gln-29 (Figure 1). This places Trp-23 almost at the end of the helix and thus in an environment substantially different from that expected for either hPTH or fragment 13–34.

Molecular Dynamics Simulations. MD simulations can provide useful information on the conformations adopted by residues in polypeptides. However, structures that represent

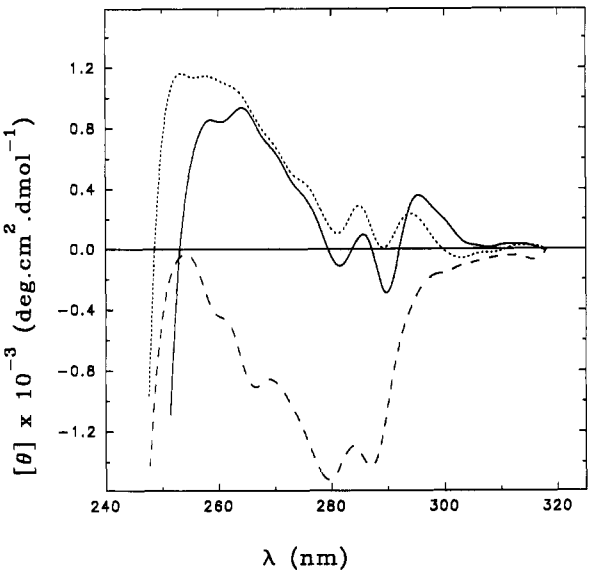

FIGURE 4: Near-UV spectra of PTH analogues. Spectra were taken in 25 mM sodium phosphate, pH 7.2, with added TFE. TFE concentrations were those at which limiting spectra were obtained. Shown are 1–84 (—) (10% TFE), 13–34 (- - -) (20% TFE), and 20–34 (— — —) (40% TFE).

an average conformation adopted by the molecule, such as those interpreted from experiments carried out at thermodynamic equilibrium, can be computed only if the simulation has reached a steady-state equilibrium (Allen et al., 1987). In the absence of knowledge about the specific equilibrium conformation of a peptide from which to construct an initial structure, it is generally not possible to carry out simulations so that a steady-state equilibrium is attained. In the work described below, various initial conformations were used for the simulations.

Different regions of conformation space were explored in simulations of fragment 20–34 starting with different conformations A (helical, $\epsilon_b = 78$), B (randomized, $\epsilon_b = 78$), C (extended, $\epsilon_b = 78$), and D (randomized, $\epsilon_b = 2$) (Table II).

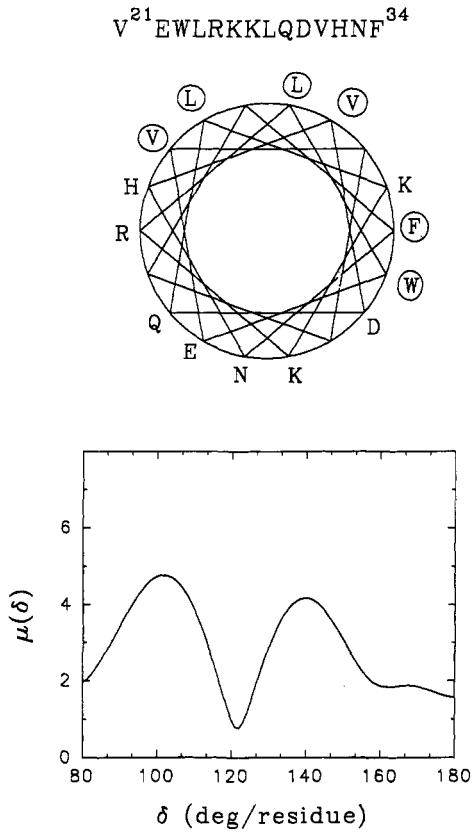

FIGURE 5: Amphiphilic region of PTH(1–34). The sequence 21–34 is shown projected onto a helical wheel (upper). The hydrophobic moment of the 21–34 (—) sequence is shown plotted as a function of the periodicity angle per residue, according to Eisenberg et al. (1984) (lower).

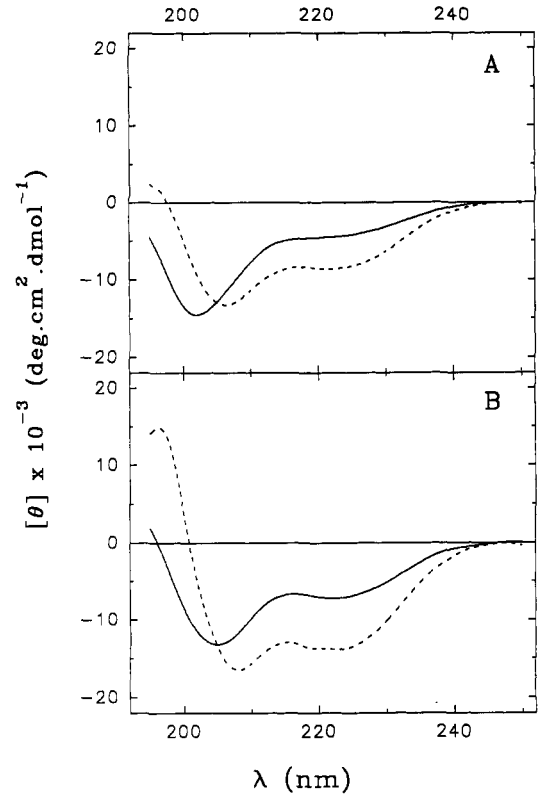

FIGURE 6: Binding of hPTH analogues to POPS. The solvent contained 20 mM Hepes, pH 7.2, and 100 mM NaCl. POPS was added to a 20:1 mole ratio of POPS to peptide. (A) 1–84 plus POPS (---); minus POPS (—). (B) 1–34 plus POPS (---); minus POPS (—).

Even after simulations of 2–3 ns, equilibrium structures were not found for 20–34 hPTH. Thus, it is even less likely that the much shorter (0.5-ns) stimulations A and B of 1–34 hPTH in Table III attained equilibrium. Nevertheless, we have used a fuzzy cluster analysis (Bezdek, 1981; Gordan & Somorjai, 1992) of the root-mean-square distances among conformations to locate clusters of similar structures accessed during a given MD trajectory. Tables II and III contain the secondary structure analysis of the conformations found to be closest to the centers of the identified clusters. The cluster centers are not average conformations but are representative of the class of polypeptide structures that comprise the cluster.

Both in a water-like (ϵ_b = 78) and in a very nonpolar (ϵ_b = 2) solvent, a large portion of 20–34 tended toward helical or helical-like conformations (Table II). Patterns of structure tend to be separated by one or more residues in the region Lys-26–Gln-29. The strongest helical indication was for the sequence Val-21–Arg-25, although this segment had no assignable structure in run C. These results are consistent with the thermodynamic prediction of a possible helix in residues 22–29 and the CD analyses in Table I. It should be emphasized, however, that the latter reflect an equilibrium situation whereas the MD simulations are at an unknown point on an approach to equilibrium.

Both simulations of 1–34 hPTH (runs A and B in Table III) were started from a fully helical conformation. In the nonpolar solvent, this helical configuration was very stable: throughout the entire 0.5-ns simulation, the fragment remained in an α-helix. In the water-like solvent, the full helical conformation was not stable. A bend defined by residues 11–19 formed. A large proportion (0.77) of the conformations in run A belong to the second cluster, whose center displays this bend and has a significant amount of helical structure surviving. The results are generally consistent with the thermodynamic prediction of possible helices in the regions 1–8 and 17–29.

Amphiphilic Regions. The sequence 1–38 was searched for possible amphiphilic regions, on the premise that such regions might relate to the biological activities of this hormone. One such region was identified, which included residues 21–35. The region 21–34 is shown projected onto a helical wheel in Figure 5. This figure also includes a plot of the hydrophobic moment versus the periodicity angle δ, calculated according to Eisenberg et al. (1984). This angle is defined, in radians, as $2\pi/m$, where m = number of residues per turn of the periodic structure. The plot shows a maximum value for δ of 100°, characteristic of an amphiphilic helix.

A notable feature of many amphiphilic peptide hormones is the ability to form complexes with phospholipids (Epand et al., 1983). Several analogues and hPTH were examined with respect to their binding to membranes of POPS, an acidic phospholipid. The far-UV spectra of hPTH and analogue 1–34, in the absence and presence of POPS vesicles (20:1 mole ratio of lipid to peptide), are shown in Figure 6. The corresponding spectra for analogues 13–34 and 20–34 are shown in Figure 7. The choice of lipid concentration in these experiments was dictated by titration data which showed that a 20-fold molar excess of POPS was sufficient to saturate the binding of each analogue (unpublished data from this laboratory). Clearly, all of the peptides containing the 20–34 sequence showed an induction of helix in the presence of the lipid. However, no lipid-induced increase in helicity was observed with fragment 1–19 (data not shown).

Estimates of the number of residues found in α-helical conformation in the presence of saturating amounts of POPS are given in Table IV. The fraction of helix observed in analogue 1–34 in the presence of POPS (about 50%) is con-

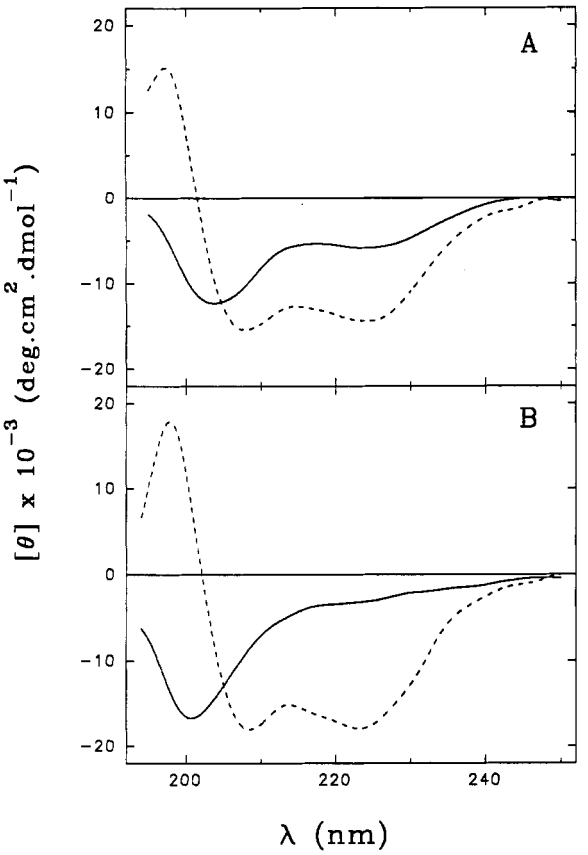

FIGURE 7: Binding of hPTH analogues to POPS. The solvent contained 20 mM Hepes, pH 7.2, and 100 mM NaCl. POPS was added to a 20:1 mole ratio of POPS to peptide. (A) 13–34 plus POPS (---); minus POPS (—). (B) 20–34 plus POPS (---); minus POPS (—).

Table IV: Helical Residues Induced by Lipid Micelles

	number of residues in α-helix[a,b]		
analogue	Hepes buffer	+POPS	increase
1–84	15	26	12
1–34	9	17	8
13–34	5	11	6
20–34	–[c]	10	6–10

[a] Helical residues were calculated as in Table I. [b] Experiments were carried out in 20 mM Hepes, pH 7.2, and 100 mM NaCl. [c] Calculated value ≤4.

sistent with the predictions from Figures 1 and 5. These predictions, together with the observation that the largest relative increase in helicity occurs for the fragment 20–34, support the notion that the helix stabilized in an interfacial environment runs from at least Arg-20 to Phe-34. However, it is worth noting that hPTH showed a slightly larger increase in helicity in the presence of the POPS than would be expected if all its amphiphilic sequence lay within the 1–34 region. In the complete hormone, the amphiphilic helix may extend farther to Leu-37.

Discussion

Circular dichroism, along with predictive algorithms and molecular dynamics simulations, has been used in this work to demonstrate regions within hPTH that have a propensity to form an α-helical structure under favorable solvent conditions. These results are summarized in Figure 8 for the important biological fragment hPTH(1–34). Although hPTH has little ordered secondary structure in aqueous buffer, helical structure is induced either by the addition of TFE or by the presence of a lipid interface. The CD data suggest that the

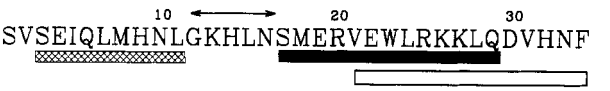

FIGURE 8: Structural elements of hPTH(1–34). The regions delineated by bars are proposed to be α-helical under different solvent conditions: Ser-3–Leu-11, cross-hatched, stable in 20–40% TFE; Ser-17–Gln-29, solid, stable in 10–20% TFE; Val-21–Phe-34, open, stable in the presence of POPS vesicles. The region of a bend is indicated by the two-headed arrow.

helix first stabilized on addition of only 10–20% TFE contains Trp-23. At this TFE concentration, fragment 13–34 has about 13 residues in an α-helical conformation. The most strongly predicted helix within hPTH is that including residues 17–29 (Figure 1). This sequence has three features which have been shown to have a high probability of occurrence in an α-helix (Richardson & Richardson, 1989). These features are the presence of a serine at the NH_2 terminus, a glutamate at position $N + 1$, and a cluster of basic residues near the COOH terminus. In addition, a potential salt bridge between Glu-22 and Arg-25 or Lys-26 could stablize this helical structure (Marqusee & Baldwin, 1987). This particular helical region is probably partially stable even in the absence of added TFE, thus accounting for the weak α-helical-like CD signal in aqueous buffer of fragment 13–34 and other analogues containing this sequence.

A second helix, 11 residues in length, is predicted from Figure 1 to be at the NH_2 terminus of hPTH. The CD data are compatible with a helix of up to 13 residues in length in fragment 1–19. This helix appears to have a slightly lower stability than that of the proposed helix within residues 17–29, since there is little evidence for its presence in the absence of TFE. However, the difference between the computed helical residues of hPTH and hPTH(8–84) in 10% TFE (Table I) suggests that the NH_2-terminal helix may be partially stable at even this low TFE concentration. MD simulations show that residues at both the NH_2 terminus and the COOH terminus tend to adopt random configurations. Thus, this helix is proposed to begin with Ser-3. The presence of a glycine at position 12 effectively requires that the helix terminate at Leu-11 (Richardson & Richardson, 1989). A region within this putative helix, Ser-3–Met-8, is predicted to have a particularly high α-helical propensity and might be expected to form some helical structure even in water. However, the well-known length dependence of the CD spectrum of α-helices (Yang et al., 1986; Manning et al., 1988) could result in a low CD signal for such a short helix, and it could go undetected in a fragment such as 1–19.

Our results concerning the structure of PTH in water or in the presence of added TFE are generally consistent with earlier predictions (Cohen et al., 1991; Zull et al., 1980). A recent study of Zull et al. (1990) suggested that the helical-like region within PTH(1–34) in neutral, aqueous buffer is located toward its NH_2 terminus. However, our results place this particular helical-like region within the 17–29 region of fragment 1–34. This is in accord with that expected from the helical thermodynamic stability profile (Figure 1). The picture presented here is also generally consistent with the structure deduced from a recent NMR and MD study of PTH(1–34) in a dilute concentration of TFE (Klaus et al., 1991). They assigned two α-helices to residues 3–9 and 17–28. Their evidence did not support the presence of a particular stable β-turn in the region of Gly-12 and Lys-13.

In addition to the potential helices that are stabilized by TFE, the present study has identified a sequence within hPTH that upon binding to a lipid interface forms an amphiphilic helix. This is a novel and particularly important finding since,

as discussed below, the presence of an amphiphilic helical structure, which appears to be confined to residues 20–34, is likely to be of a direct biological relevance.

The present data shed new light on the structure–function relationship in parathyroid hormone and its bioactive fragments. The entire region 1–34 has been shown to be essential for the stimulation of adenylate cyclase activity in rat osteosarcoma and kidney cells (Jüppner, 1989; Rabbani et al., 1990). This suggests that both putative α-helices in the 1–34 region could be important for the binding to the receptor associated with this activity. On the other hand, binding to the receptor(s) linked to some other major functions of PTH appears to be associated with the sequence in the COOH-terminal half of the 1–34 region. Thus, recent experiments indicate that the domain of hPTH responsible for stimulation of membrane-associated protein kinase C lies within the 20–34 region, with the terminal six residues being most essential (Jouishomme et al., 1992). A similar region has been shown to be essential for stimulation of DNA synthesis in chondrocytes (Schlüter et al., 1989) or osteoblasts (Sömjen et al., 1990) and for subsequent proliferation of these cells. All these activities are most likely linked to an as yet unidentified receptor that is independent of the receptor site associated with the cAMP pathway. In this context, we attach particular significance to the present finding that the functionally essential 20–34 region of hPTH has a high affinity for membrane lipids and folds in a membrane environment into amphiphilic α-helices. Amphiphilic helices and lipid affinity have been recognized as important features of some other biologically active peptides (Kaiser & Kézdy, 1987). The lipid phase of target cell membranes may facilitate the accumulation of the hormone near the receptor site (Sargent & Schwyzer, 1988). Furthermore, an amphiphilic helix may be an essential structural feature that promotes the actual receptor recognition of the hormone.

The question arises as to whether the sequences of PTH from other species contain similar potential amphiphilic helices. This region is highly conserved in mammalian PTHs. The sequence of bovine (Kronenberg et al., 1979) and porcine (Sauer et al., 1974) PTH is identical to that of the human in this region. Examination of the rat sequence (Heinrich et al., 1984) showed that it is also amphiphilic as judged by its corresponding helical wheel and its maximum in the hydrophobic moment plot at a periodicity angle of 100°. The chicken sequence has a somewhat lower hydrophobic moment, with a maximum value at 95°. We therefore believe that there is a strong possibility that the amphiphilic helix is important to the cAMP-independent receptor. Our current work is being focused on specific amino acid substitutions in this amphiphilic region and correlating any structural changes to effects on the biological activities.

ACKNOWLEDGMENTS

We thank J. Barbier and D. Zahab for technical assistance. We also thank Dr. D. Schomburg for providing us with a copy of his manuscript prior to publication.

REFERENCES

Allen, M. P., & Tildesley, D. J. (1987) *Computer Simulation of Liquids*, Clarendon Press, Oxford.

Bandekar, J., Evans, D. J., Krimm, S., Leach, S. J., Lee, S., McQuie, J. R., Minasian, E., Némethy, G., Pottle, M. S., Scheraga, H. A., Stimson, E. R., & Woody, R. W. (1982) *Int. J. Pept. Protein Res. 19*, 187–205.

Bezdek, J. C. (1981) *Pattern Recognition with Fuzzy Objective Function Algorithms*, Plenum Press, New York.

Brooks, B. R., Bruccoleri, R. E., Olafson, B. D., States, D. J., Swaminathan, S., & Karplus, M. (1983) *J. Comput. Chem. 4*, 187–217.

Bundi, A., Andreatta, R. H., & Wüthrich, K. (1978) *Eur. J. Biochem. 91*, 201–208.

Chou, P. Y., & Fasman, G. D. (1974) *Biochemistry 13*, 211–222.

Chou, P. Y., & Fasman, G. D. (1977) *J. Mol. Biol. 115*, 135–175.

Cohen, F. E., Strewler, G. J., Bradley, M. S., Carlquist, M., Nilsson, M., Ericsson, M., Ciardelli, T. L., & Nissenson, R. A. (1991) *J. Biol. Chem. 266*, 1997–2004.

Eisenberg, D., Weiss, R. M., & Terwilliger, T. C. (1984) *Proc. Natl. Acad. Sci. U.S.A. 81*, 140–144.

Epand, R. M., Epand, R. F., Orlowski, R. C., Schlueter, R. J., Boni, L. T., & Hui, S. W. (1983) *Biochemistry 22*, 5074–5084.

Epand, R. M., Epand, R. F., Hui, S. W., He, N. B., & Rosenblatt, M. (1985) *Int. J. Pept. Protein Res. 25*, 594–600.

Fields, G. B., & Noble, R. L. (1990) *Int. J. Pept. Protein Res 35*, 161–241.

Goltzman, D., Peytremann, A., Callahan, E., Tregear, G. W., & Potts, J. T., Jr. (1975) *J. Biol. Chem. 250*, 3199–3203.

Gordon, H. L., & Somorjai, R. L. (1992) *Proteins* (in press).

Heinrich, G., Kronenberg, H. M., Potts, J. T., Jr., & Habener, J. F. (1984) *J. Biol. Chem. 259*, 3320–3329.

Hendy, G. N., Kronenberg, H. M., Potts, J. T., Jr., & Rich, A. (1981) *Proc. Natl. Acad. Sci. U.S.A 78*, 7365–7369.

Høgset, A., Blingsmo, O. R., Saether, O., Gautvik, V. T., Holmgren, E., Hartmanis, M., Josephson, S., Gabrielsen, O. S., Gordeladze, J. O., Alestøm, P., & Gautvik, K. M. (1990) *J. Biol. Chem. 265*, 7338–7344.

Hong, B-S., Yang, M. C. M., Liang, J. N., & Pang, P. K. T. (1986) *Peptides 7*, 1131–1135.

Jouishomme, H., Whitfield, J., Chakravarthy, B., Durkin, J. P., Isaacs, R. J., MacLean, S., Neugebauer, W., Willick, G., & Rixon, R. H. (1992) *Endocrinology* (in press).

Jüppner, H. (1989) *Peptide Hormones as Prohormones: Processing, Biological Activity, Pharmacology* (Martinez, J., Ed.) pp 325–354, John Wiley, New York.

Kaiser, E. T., & Kézdy, F. J. (1987) *Annu. Rev. Biophys. Biophys. Chem. 16*, 561–581.

Klaus, W., Dieckmann, T., Wray, V., Schomburg, D., Wingender, E., & Mayer, H. (1991) *Biochemistry 30*, 6936–6942.

Kronenberg, H. M., McDevitt, B. E., Majzoub, J. A., Nathans, J., Sharp, P. A., Potts, J. T., Jr., & Rich, A. (1979) *Proc. Natl. Acad. Sci. U.S.A. 76*, 4981–4985.

Lee, S. C., & Russell, A. F. (1989) *Biopolymers 28*, 1115–1127.

Manning, M. C., Illangasekare, M., & Woody, R. W. (1988) *Biophys. Chem. 31*, 77–86.

Marqusee, S., & Baldwin, R. L. (1987) *Proc. Natl. Acad. Sci. U.S.A. 84*, 8898–8902.

O'Neil, K. T., & DeGrado, W. F. (1990) *Science 250*, 646–651.

Potts, J. T., Jr., Tregear, G. W., Keutmann, H. T., Niall, H. D., Sauer, R., Deftos, L. J., Dawson, B. F., Hogan, M. L., & Aurbach, G. D. (1971) *Proc. Natl. Acad. Sci. U.S.A. 68*, 63–67.

Rabbani, S. A., Kaiser, S. M., Henderson, J. E., Bernier, S. M., Mouland, A. J., Roy, D. R., Zahab, D. M., Sung, W. L., Goltzman, D., Hendy, G. N. (1990) *Biochemistry 29*, 10080–10089.

Richardson, J. S., & Richardson, D. C. (1989) *Prediction of Protein Structure and the Principles of Protein Conformation* (Fasman, G. D., Ed.) pp 1–98, Plenum Press, New York.
Rink, H. (1987) *Tetrahedron Lett. 28*, 3787–3790.
Sargent, D. F., & Schwyzer, R. (1986) *Proc. Natl. Acad. Sci. U.S.A. 83*, 5774–5778.
Schlüter, K.-D., Hellstern, E., Wingender, E., & Mayer, H. (1989) *J. Biol. Chem. 264*, 11087–11093.
Seitz, P. K., Nickols, G. A., Nickols, M. A., McPherson, M. B., & Cooper, C. W. (1990) *J. Bone Miner. Res. 5*, 353–359.
Sieber, P. (1987) *Tetrahedron Lett. 28*, 2107–2110.
Smith, L. M., Jentoft, J., & Zull, J. E. (1987) *Arch. Biochem. Biophys. 253*, 81–86.
Sömjen, D., Binderman, I., Schlüter, K.-D., Wingender, E., Mayer, H., & Kaye, A. M. (1990) *Biochem. J. 272*, 781–785.
Stewart, J. M., & Young, J. D. (1984) *Solid Phase Peptide Synthesis*, 2nd ed., pp 1–40, Pierce Chemical Co., Rockford, IL.
Strickland, E. H. (1974) *CRC Crit. Rev. Biochem. 2*, 113–175.
Sung, W. L., Zahab, D. M., Barbier, J. R., Watson, D., Yaguchi, M., Neugebauer, W., & Willick, G. E. (1991) *J. Biol. Chem. 266*, 2831–2835.
van Gunsteren, W. F., & Berendsen, H. J. C. (1977) *Mol. Phys. 34*, 1311–1327.
Woody, R. W. (1985) *The Peptides* (Hruby, V. J., Ed.) Vol. 7, pp 15–104, Academic Press, New York.
Yang, J. T., Wu, C.-S., & Martinez, H. (1986) *Methods Enzymol. 130*, 208–269.
Zull, J. E., & Lev, N. B. (1980) *Proc. Natl. Acad. Sci. U.S.A. 77*, 3791–3795.
Zull, J. E., Smith, S. K., & Wiltshire, R. (1990) *J. Biol. Chem. 265*, 5671–5676.

Hydrophobic Carriers of Vanadyl Ions Augment the Insulinomimetic Actions of Vanadyl Ions in Rat Adipocytes

Yoram Shechter,*,‡ Assia Shisheva,‡ Rachel Lazar,§ Jacqueline Libman,§ and Abraham Shanzer*,§
Departments of Hormone Research and Organic Chemistry, The Weizmann Institute of Science, Rehovot 76100, Israel
Received July 31, 1991; Revised Manuscript Received November 4, 1991

ABSTRACT: A novel family of vanadyl ion (VO^{2+}, oxidation state +4) carriers is introduced. These carriers possess C_2 symmetry, utilize two hydroxamate groups as ion binding sites, and optionally possess asymmetric carbons. Binding efficiencies and hydrophobicities are regulated by the use of a modular assembly. When applied to rat adipocytes, these carriers augment the potency of vanadyl ions to stimulate glucose metabolism. The complexes shift the dose–response curve to the left. Also, the maximal effect of vanadyl ions which is in the order of 20–30% of that of insulin is shifted toward maximal (100–115%) stimulation. Among several chelators studied, the order of synergistic potency was RL-252 ≥ RL-262 > 1367. RL-239, RL-280, and RL-261 had smaller effects, whereas RL-282 had a negligible effect. The synergistic action of RL-252 (and other chelators as well) on VO^{2+} was already observed at a molar ratio of 1:0.01 of VO^{2+} to RL-252, respectively, and maximal augmentation occurred at a molar ratio of 1:0.1. The superiority of the hydrophobic chelators relative to the hydrophilic ones, together with the low molar ratio of chelator to VO^{2+} to achieve maximal effect, strongly suggests that these chelators act as vanadyl ionophores. This notion was confirmed by carrier-facilitated extraction of VO^{2+} from water into $CHCl_3$ with the following order of decreasing efficacy: RL-262 > RL-252 > 1367 > RL-261. The chelators' potentiating effect may therefore be related to facilitated transport of VO^{2+} ions into the cells' interiors. The potency of vanadate ions (VO_3^-, oxidation state +5) was not increased by RL-252, although RL-252 proved to extract vanadate effectively from water into chloroform. This observation is in line with earlier findings that vanadyl ions, rather than vanadate ions, are the activating principle, and suggests that the effectiveness of vanadate is dependent on the cells' capability to reduce it to vanadyl ions. Vanadyl ions, on the other hand, do not require intracellular reduction events. Their limited solubility at neutral pH value and low permeability is now full overcome by the ionophores which facilitate their permeation at low concentrations of the cation. Moreover, the substantially lower potentiating effect of the D-isomer, RL-262 (D), than of the L-isomer, RL-262 (L), suggests that the vanadyl ions exert their function by interactions with chiral recognition sites. The clinical significance of this study is also discussed.

Intensive research carried out in the last decade has demonstrated that vanadate ions, (VO_3^-, oxidation state +5) and also vanadyl ions (VO^{2+}, oxidation-state +4) (Shechter & Karlish, 1980), mimic nearly all of the various actions attributed to insulin in a large variety of in vitro (cellular) systems (Tamura et al., 1984; Shechter, 1990). Thus, VO_3^- and VO^{2+} may be considered as wide-range insulin-mimicking agents. A new interest in vanadium emerged in 1985 when Heyliger et al. observed that vanadate ions administered orally (in drinking water) to streptozotocin-treated hyperglycemic rats reduced the high levels of circulating glucose down to normal values and ameliorated many of the aberrations induced by hyperglycemia (Heyliger et al., 1985; Meyerovitch et al., 1987). In addition, disorders not directly related to

* Authors to whom correspondence should be addressed.
‡ Department of Hormone Research.
§ Department of Organic Chemistry.

0006-2960/92/0431-2063$03.00/0